VELOCITY AND DENSITY FIELD MEASUREMENTS OF A MICRO-EXPLOSION

L. VENKATAKRISHNAN[1c], P.SURIYANARAYANAN[1], G. JAGADEESH[2]

[1]Council of Scientific and Industrial Research-National Aerospace Laboratories, Bangalore, 560012, India
[2]Department of Aerospace Engineering, Indian Institute of Science, Bangalore, 560037, India

[c]Corresponding author: Tel.: +918025051566; Fax: +918025051677; Email: venkat@nal.res.in

KEYWORDS:
Main subjects: Blast Waves, flow visualization
Fluid: high speed flows, flows with shocks
Visualization method(s): Background Oriented Schlieren, Particle Image Velocimetry
Other keywords: image processing, tomography,

ABSTRACT: This paper describes the implementation of Background oriented Schlieren (BOS) technique to capture the density field of a blast wave generated through a micro-explosion. The three dimensional density field was reconstructed using the filtered back projection technique. This was carried out at several instants of time in order to capture the evolution of the density field. The reconstructed density field revealed the internal structure of the flow field. The results show that there is a significant variation in density between the forward and rearward propagating parts of the shock wave. This implies that these micro-explosions possess some characteristics similar to a muzzle blast rather than a true point source. PIV measurements were also attempted at several instants of time. However, the alumina particles expelled from the tube had very high S/N ratio resulting in saturation of the CCD. Hence no useful velocity field data could be obtained. The density fields generated in this study helps to understand the flow physics associated with blast waves generated using controlled micro-explosions. The findings can be used to scale laboratory experiments to real life explosions.

1 Introduction

Energy released by the detonation of high explosives or a mixture of volatile gases causes significant increase in the dynamic pressure caused due to the acceleration of the source gases (Dewey [5]). This sudden release of energy forms a supersonic shock front, when expansion exceeds the ambient sound speed. This shock front is characterized by exponential type decay of its properties, immediately after reaching a peak. Unlike shock waves that attenuate as they expand spherically; the shock wave from an internal blasts can change its propagation properties depending on the physical barriers (Baker [3]; Kenny and Graham [4]).The physical property of the blast wave depends on the rate of energy release and the amount of explosives used for detonation. The energy released by detonation of such high explosives calculated based on theoretical chemical analysis (Dewey [6]) may not be valid in predicting the physical properties of the blast waves generated by it. This is due to the fact that the chemical process involved in such detonation forms many by-products and it makes extremely difficult to quantify the absolute amount of energy released during the process. The alternate way in determining the relative energy released by an explosive is to measure the center of the explosion at which specific property of the blast wave property occurs and then compare it with distance at which same property produced by a TNT explosion of equivalent mass using cube root scaling law (Kliene et al. [12]; Dewey [7]; Hargather and Settles [9]). Dewey [8] has shown that shock wave radius and overpressure as a function of time gives better characterization about nature of the explosive instead of TNT equivalence alone. This emphasizes the importance of studying blast waves experimentally to characterize their physical properties.

Blast wave propagation from large-scale blasts was studied by Dewey [4-8]. Recent efforts such as Sommersel et al. [14] who carried out a hydrogen gas explosion test and Mizukaki et al. [15] who used C-4 high explosives and EMX emulsions have been focused on large scale tests to characterize the blast wave for its overpressure values. Determination of shock wave propagation from large scale blasts is cumbersome, expensive, laborious and time-consuming and imposes limitations on applied diagnostics. Small scale explosions or small sized charges offer advantages, as they can be economical, safely used and less time – consuming in the laboratory environment. The characterization of the small scale tests of a given mass for radius and thermodynamic properties can be scaled for

explosives using Hopkinson's scaling laws, pioneered by Kliene et al. [12] for milligrams sized charges. This paves the way for the use of micro-explosion/small scale blast as an experimental tool for a qualitative study of the large scale blast waves, within the laboratory.

The generation of blast waves in the laboratory has been achieved through a variety of means. Jiang et al. [11] used laser to deposit energy within a small region (point source of energy), Kleine et al. [12] generated blast waves from milli-gram silver azide charges and extended the scaling laws for the gram sized charges. Hargather et al. [9] has generated the micro-blast waves by ignition/detonation of gram sized explosive charges and Murphy et al. [13] used exploding bridge wires to generate laboratory scale explosions and measured the velocity of the blast wave using PIV.

Measurements of spherical blast waves are complicated as the flow is non-isentropic and in order to describe all the thermodynamic properties, properties like over pressure, density and velocity have to be measured independently. Due to the transient non-stationary nature of the flow, the application of any flow diagnostic technique is quite challenging. Additionally the quantitative determination of the density field remains a challenge.

In earlier approaches the relationship between arrival time of the shock and the shock radius obtained from high speed imaging was used to obtain the shock velocity by using either a non-linear least square or power curve fitting. The thermodynamic properties are then obtained by application of Rankine-Hugonoit equations. The density field while highly informative is quite difficult to capture in a flow like micro-explosion. In a laboratory, density can be measured directly using laser interferograms and laser absorption. However these techniques are cumbersome in measurement and time consuming to obtain the quantitative density fields. The Background Oriented Schlieren (BOS) technique provides the capability of capturing three dimensional density fields (Venkatakrishnan and Meier 2004; Venkatakrishnan and Suriyanarayanan [20]). Sommersel et al. [14] and Mizukaki et al. [15] have used the BOS technique on large and laboratory scale blasts respectively; however no quantitative density field could be obtained. This is an attempt to quantify the density flow field of a micro-explosion for the first time using the BOS technique.

In this study, a micro-explosion is generated using NONEL tube (Obed et al. [17]) and a detonating device. The spatio-temporally evolving density field is captured at several instants by means of a precise triggering circuit used to control the illumination and imaging. The density field so obtained can be used for both understanding basic physics associated with explosive driven shock wave propagation as well as provide data for validation of CFD attempts to model such flows.

2 Experimental procedure

2.1 Micro-explosion generator

The micro-explosion is generated at the open end of a non-electrical (NONEL®) tube (M/s Dyno Nobel, Sweden), an explosive transfer system. The system consists of a plastic tube of approximately 1.8 mm inner diameter and 3 mm outer diameter with a thin layer of explosive material coating (HMX with traces of aluminum 18 mg/m length of the polymer tube) deposited on its inner wall of the tube. The ignition of the NONEL® tube was done using NONEL Dynostart®, an electronic blasting device in which electrical energy is converted into a powerful spark. It consists of an energy source (battery), a voltage converter, a capacitor for energy accumulation (2500V approx), an electrode and push buttons to effect initiation. The electrode emits a spark into the inner surface of the NONEL® tube to initiate the ignition of the explosive coating.

The ignition of the reactive material coated on the inner surface of the NONEL® tube results in the formation of a combustion wave. The combustion wave also heats up the gases in the tube. The dispersed energetic material is heated and then combusted to release energy which supports the shock front at a typical rate of 2000 m/s. The detonation is confined to the plastic tube along its length and the products of combustion are allowed to escape from the open end of the tube. These products of combustion are at higher pressure than the ambient and due to its sudden expansion at the open end results in the formation of a blast wave.

2.2 Background Oriented Schlieren (BOS) methodology

The principle of the technique is the refractive index variation due to density gradients in the flow. The determination of the density field using BOS thus involves the following steps: (a) calculation of displacements in the background which is imaged through the flow of interest. This is done through a PIV-type cross-correlation algorithm. These displacements are the vectors of density gradient at each point; (b) calculation of the line-of- sight integrated density

field by solution of the Poisson equation, which is the gradient of the above displacement; (c) use of optical tomography (filtered back-projection) to determine the density field in the actual plane of interest. The reader is referred to Venkatakrishnan and Meier (2004) for a derivation of the reconstruction function. The reconstruction of the entire density field is achieved by inverse tomography (Venkatakrishnan and Suriyanarayanan, [20]).

2.3 Experimental setup

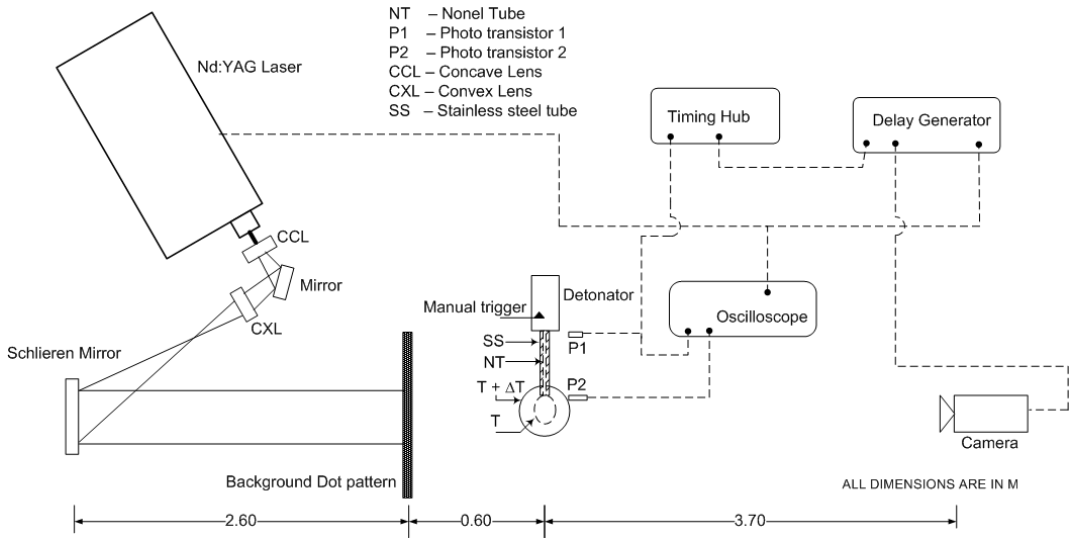

Figure 1: Schematic of the experimental setup

The micro-explosion was captured initially using a Motion pro X3 (1280 x 1024pix), 1MP camera. In subsequent experiments a Motion pro Y5 (2336 x 1728pix), 4MP camera was used to increase the spatial resolution of the flow being imaged. The area of imaging was 220 x 180mm with X3 and 250 x 200mm with Y5 camera. A Nikon 300mm lens is used for imaging. The data being presented here are from Y5 camera unless otherwise mentioned. While conventional BOS consists of a steady light source, the present experiment requires exceedingly short exposure time due to the non-stationary nature of the flow. Hence an Nd:YAG pulsed laser 400mJ with a pulse width of 10ns was used as illumination source. The speckling effect of the laser was removed by using an optical grade translucent filter after expanding the beam using a concave lens. In order to obtain the time evolution of the blast, multiple runs were required. A trigger preset to specific time instants after the blast initiation was used. The timing circuit is explained in the next section. IDT proVISION-XS® software was used for image acquisition and cross-correlation of the flow image with the background to obtain the displacement field, which is also the density gradient field. The dot pattern used for the study has a resolution of 1800 dpi. Oommen et al. [16] showed that the NONEL tube gave good repeatability for length beyond 225mm. In the present experiments the NONEL® tube was always cut to a length of 230mm and inserted into a stainless steel (SS) tube of inner diameter 3mm as shown in the Figure 1. Two photo diodes P1 and P2 (as shown in Figure 2) were used to get the instants of time at which the spark was initiated inside the NONEL® tube and the combustion products

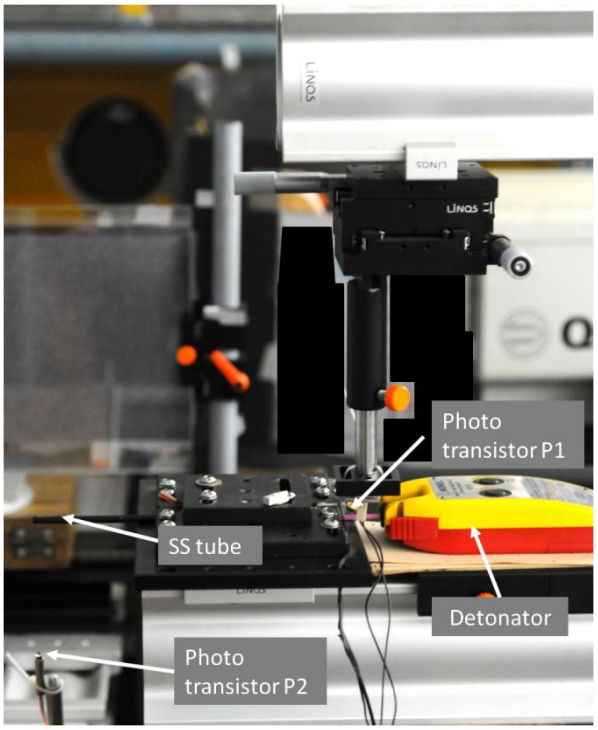

Figure 2: SS tube holding the NONEL tube and location of photo diode

exiting from the NONEL® tube. The background was kept at a distance of 3.7 m from the camera and 0.6 m from the background. The aperture was kept at a minimum to increase the depth of focus. This was done to keep both the background dot pattern and the flow in focus. The spatial resolutions were 3mm for the X3 and 1.82mm for the Y5 camera respectively. The experimental set up was erected on a rigid support system made of LINOS® X-rail components to allow precise alignment of the components and isolate the blasting device so as to prevent any unwanted vibration due to the blast.

2.4 Timing circuit

The image acquisition software was synchronized with the timing hub, the camera and the laser with a delay using a Stanford Research systems delay generator DG 535 to capture the spatio-temporally evolving blast wave. Signal traces from the two photo diodes (P1 and P2), and laser (Q) switches were recorded in the oscilloscope to capture initiation of

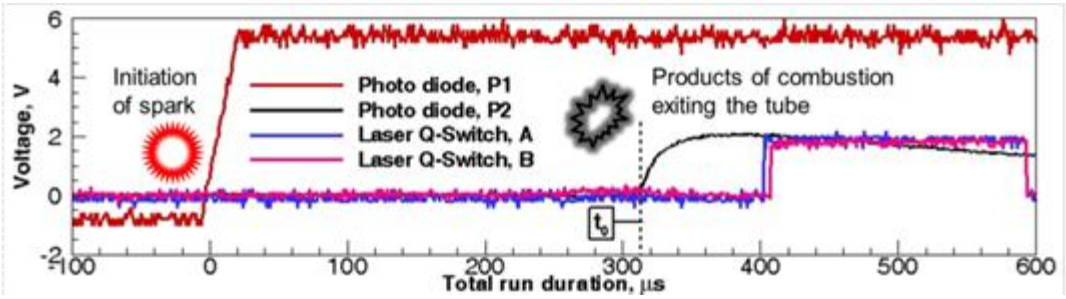

Figure 3: Trace captured during a run

the blast wave being captured as shown in Figure 3. Depressing the Dynostart® firing button initiates the spark which ignites the explosive material coated inside the tube. This spark was picked up by the photo-transistor P1 and this signal was used to trigger the Motion pro® timing hub. The time taken for the flow to come out of the tube after ignition was 115µs and the combustion products exit from the tube with a bright white light. The instant of time at which the flash exits the tube is taken as t_0 and this is picked up by the second photo diode P2. The difference in time between the firing of the laser Q switches and t_0, gives the time information of growth of the blast wave.

2.5 PIV experimental setup

The camera and the laser used for the BOS experiments were used in PIV experiments also. The laser light sheet was formed at the downstream of the direction of propagation of the blast wave. The schematic of the PIV setup is shown in Figure 4. The sheeting optics was kept at a safe distance so that the sheet optics does not vibrate due to the impact of the

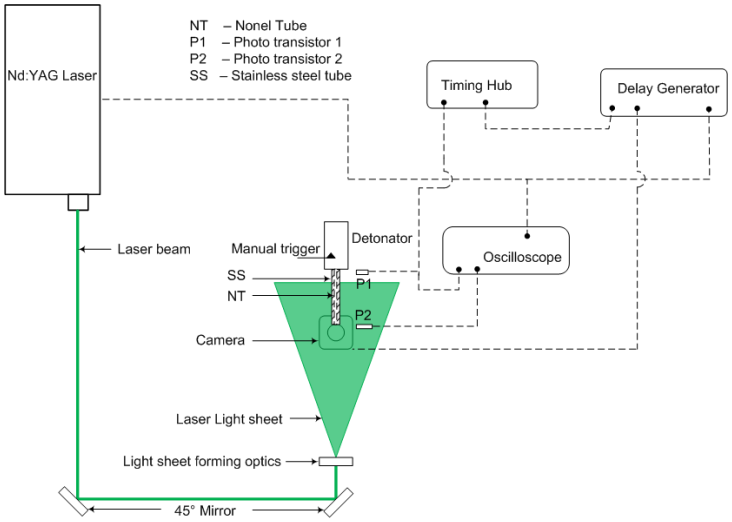

Figure 4. Schematic of the PIV experimental setup

blast wave. The thickness of the laser sheet formed was 0.8mm. The ambient was seeded using the particles generated

from the nebulizer which uses ethylene glycol based liquid. The area surrounding the SS tube was barricaded with the chart papers to create uniform seeding of particles in the ambient of the blast wave. A green filter was used to allow only laser light and filter out high intensity flash created due to the products of combustion at the exit of the tube. The experiments were carried out using the same timing circuit as used for the BOS.

3 Results and Discussion

3.1 BOS measurements

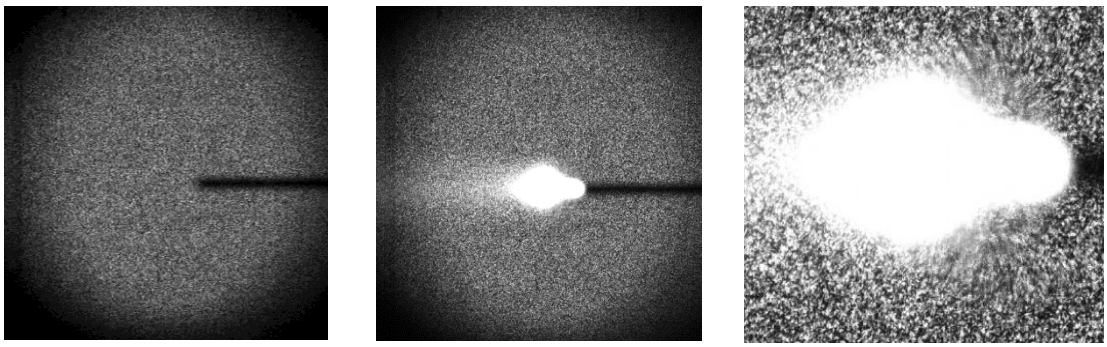

Figure 5. Background dot pattern in (a) no-flow (b) flow condition and (c) close-up of (b)

The Figure 4 shows the image of the background at no-flow condition and after the initiation of the detonation. In order to eliminate the random noise present due to air currents in the laboratory, 20 background images were taken each before and after the flow and correlated with the flow condition to average out the random fluctuations. Figure 5 shows three realizations of the background with (a) no flow, (b) flow and (c) a close-up of the tube exit. While Figure 5a and Figure 5b look similar as expected (prior to correlation which would reveal the shock), a close-up of the nozzle exit (Figure 5c) shows the large streaky distortion of the background which is caused due to the highly turbulent nature of the flow exiting the tube. Despite the background illumination being limited to the laser pulse width of 10ns, the illumination caused by the products of combustion (muzzle flash) lingers over several tens of microseconds and causes a loss of data in that region. The camera exposure for BOS was 70µs when compared to that of 500ns exposure used in the high speed Schlieren imaging. The flash at the core persists for longer duration in BOS experiments than the Schlieren and this causes loss in data in those regions.

The data are processed in the standard PIV fashion using IDT's proVISION-XS® software with the interrogation region set to 16 x 16 pixels in the adaptive mode. Since the flow in the present study is continuously expanding the same grid density was maintained across all cases to enable suitable comparison. Figure 6 presents the vector field of the

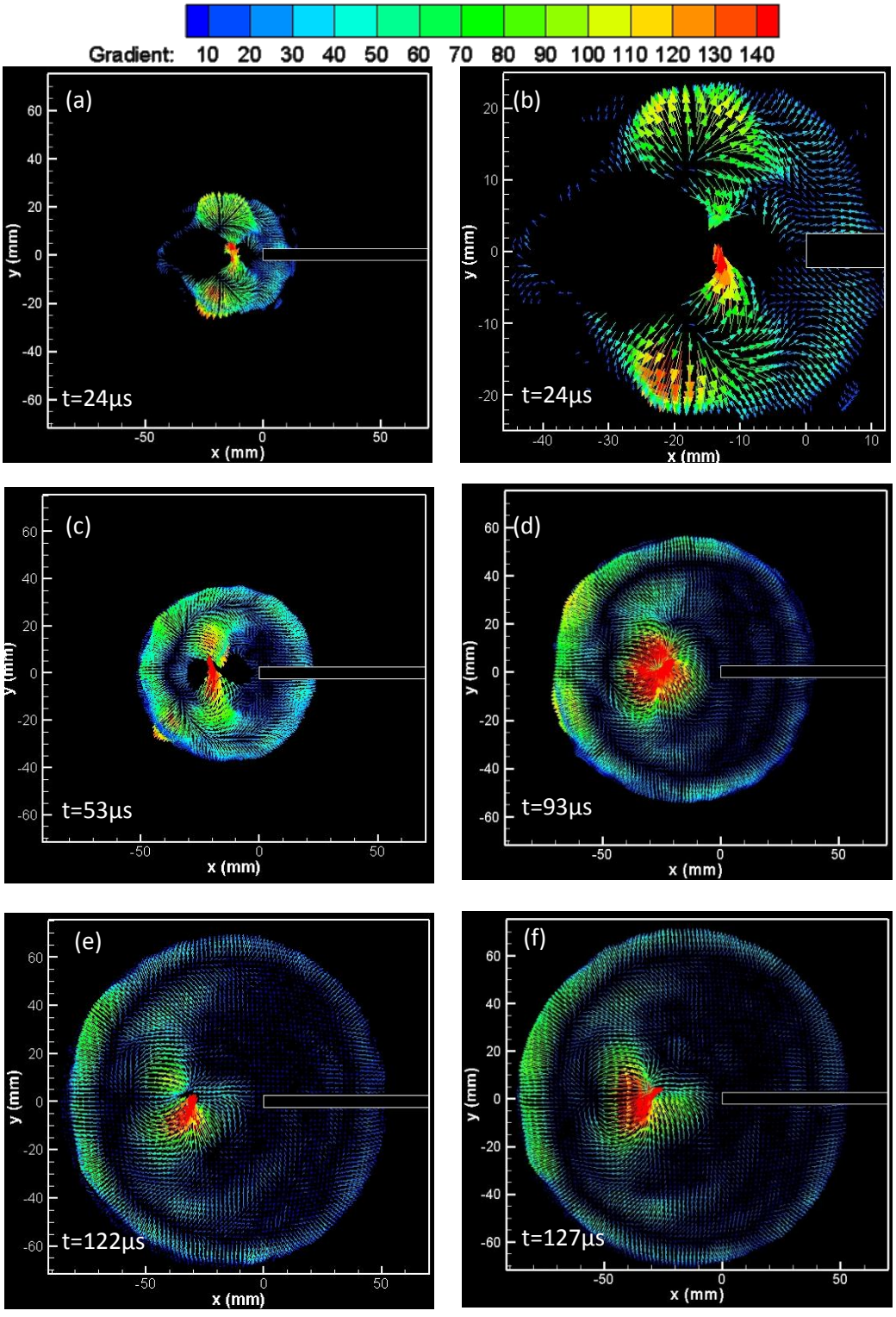

Figure 6: Displacement field corresponding to density gradient field at different time instants showing evolution of blast wave.

displacements so obtained at several time instants.

These displacements correspond to the bi- integrated density field and are such, equivalent to bi-directional Schlieren. The vectors point in the direction of higher density and are color coded to the strength of the bi-directional gradient shown in arbitrary units. The holes in the vector field represent the blanked out regions corresponding to the saturation caused by the muzzle flash. The figure shows that growth and evolution of the blast wave is well captured using the BOS technique. Figure 6a is the gradient field for the condition shown in Figure 5 and is also presented in a close-up in Figure 6b. It is illuminating to compare this to Figure 6g which is a single frame of a time resolved (500kHz) Schlieren (Obed et al. [17]) obtained for an identical flow. The comparison clearly shows the initial shock formation at the tube exit partially obscured by the muzzle flash. However, the comparatively small time resolution (2μs) and low spatial resolution of the high speed camera is unable to resolve the turbulent structure within the blast wave. This internal structure is seen very clearly even in the line-of-sight integrated gradients which are presented in Figure 6b. Kliene et al. [12] has shown that the micro-explosions have an asymmetric shape during the initial phase of the blast wave formation. However from the gradient field, it is difficult to pronounce whether the initial shape of the blast wave in the present case is like that shown by Kleine et al. [12] due to the flash. The reconstruction of the density field from BOS presented in the subsequent section will help to clarify this issue.

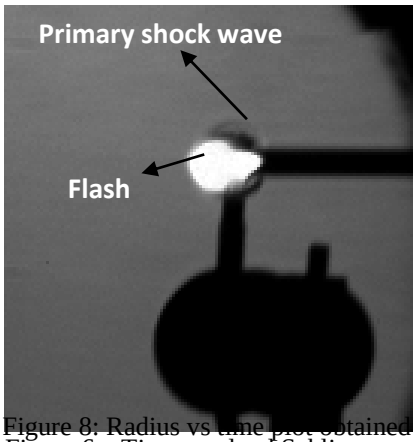

Figure 8: Radius vs time plot obtained from Figure 6g. Time resolved Schlieren at BOS. instant t=24μs showing shock front.

3.1.2 Schlieren image construction from BOS

As pointed out earlier, the displacement field corresponds to bi-directional Schlieren. The magnitude of this field can

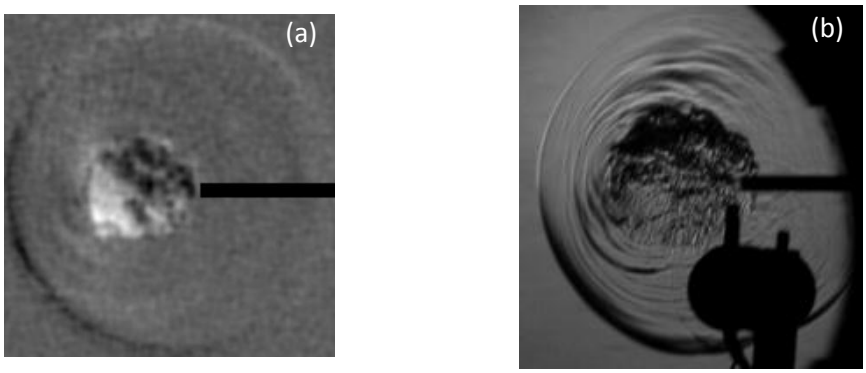

Figure 7: (a) Bi-directional Schlieren image reconstructed from the BOS, (b) Schlieren image at t = 127μs

thus be used to create a gray scale image. The figure 7 shows the bi-directional Schlieren image constructed at time t = 127μs. The images show that the highly turbulent density field in the core of the blast wave has been captured. Comparison with a regular high speed Schlieren shown in Figure 7b for the same flow (Obed et al. [17]) show there is a close resemblance of the flow features.

3.1.3 Blast wave radius determination using BOS

In order to obtain the evolution of the blast wave with time, the radius of the blast wave for each time instant was calculated. A circle was fitted to the bi-directional density gradient field to determine the radius at different time instants. Figure 8 shows the spatio-temporally growing blast wave radius obtained from the BOS measurements at different times. The plot contains data obtained from both the cameras and emphasizes the repeatability of the experiments.

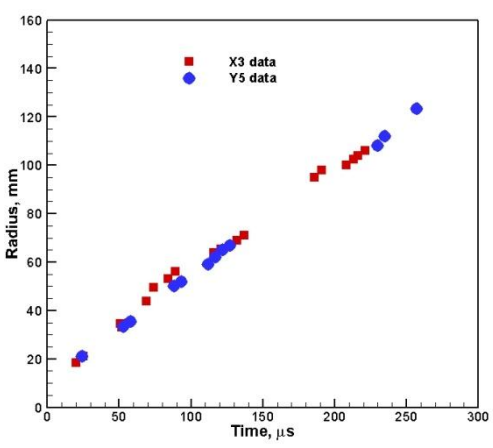

3.1.4 Scaling analysis

Oommen et al. [16] measured the overpressures at different downstream distances (from the exit of the NONEL® tube). They were found to be

identical irrespective of the length of the tube used for generating the blast suggesting a fixed amount of explosive responsible for the energy yield at the tip. They calculated the weight of explosive in TNT equivalent weight was estimated. The TNT equivalent weight for the NONEL® tube was found to be 1.63 mg.

The scaling laws for the small gram sized explosives was given by Kliene et al. [12], accounts for temperature and pressure differences in atmospheres in to which the charges detonate. The scaling equations are given in Eq. 1 and Eq. 2.

$$R_S = \frac{R}{S} \qquad t_S = \frac{c*t}{S} \tag{1}$$

$$S = \left(\frac{W}{W_{TNT}}\right)^{(1/3)} * \left(\frac{101.325}{P}\right)^{(1/3)} \qquad c = \left(\frac{T}{288.16}\right)^{(1/2)} \tag{2}$$

where,

R – Measured radius of the blast wave through BOS in mm.
t – Time captured from the trace in µS.
R_s – Radius scaled to standard TNT explosive in mm.
t_s – Time scaled to standard TNT explosive in µS.
S & c – Scaling parameters at Normal Temperature and Pressure (NTP).
T & P – Temperature and pressure during the detonation respectively.
The resulting radius and time is then fitted with an equation of the form as given by Dewey [5]. A, B, C and D are the coefficients obtained through the curve fit and a_0 is the speed of sound at NTP.

$$R_S = A + Ba_0t_S + C\ln(1+a_0t_S) + D\sqrt{\ln(1+a\,t_S)} \tag{3}$$

A non -linear least squares fit was used to obtain the coefficients of the equation. However there are some constraints which have to be applied during the curve fit. Coefficient B in Eq. 3 should be set to 1, so that the Eq. 3 asymptote to the speed of sound for large time. Shock Mach number, M_S is obtained by taking the time derivative of the Eq. 3.

$$M_S = \frac{dR_S/dt_S}{a_0} = \left(1 + \frac{C}{1+a_0t_S} + \frac{D}{2(1+a_0t_S)\sqrt{\ln(1+a_0t_S)}}\right) \tag{4}$$

Eq. 4 is used to obtain the shock Mach number and other thermodynamic properties like over pressure and the over density are obtained from shock Mach number.

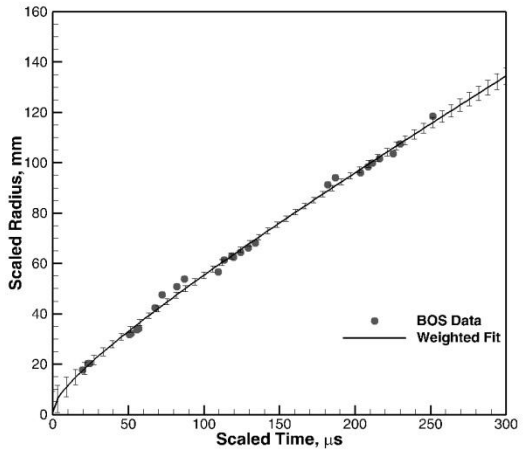

Figure 9. Curve fit using power law for scaled radius and time

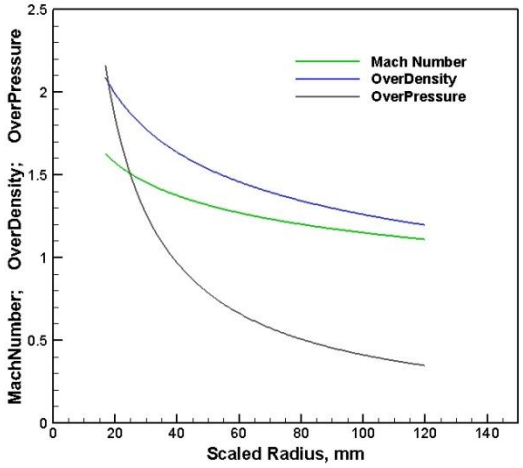

Figure 10. Mach number, OverPressure and OverDensity obtained through R-H relations

The thermodynamic properties behind the shock wave in terms of the shock Mach number was given by Dewey [5] using the Rankine-Hugoniot (R-H relation) relationships which are valid for the specific heat ratio of γ = 1.4. The over pressure and over density are given by Eq. 5 and Eq. 6 respectively.

$$\frac{\rho_S}{\rho_0} = \frac{(\gamma+1)M_S^{\,2}}{(\gamma-1)M_S^{\,2}+2} = \frac{6M_S^{\,2}}{M_S^{\,2}+5} \qquad (5)$$

$$\frac{P_S}{P_0} - 1 = \frac{2\gamma}{\gamma+1}\left(M_S^{\,2}-1\right) = \frac{7}{6}\left(M_S^{\,2}-1\right) \qquad (6)$$

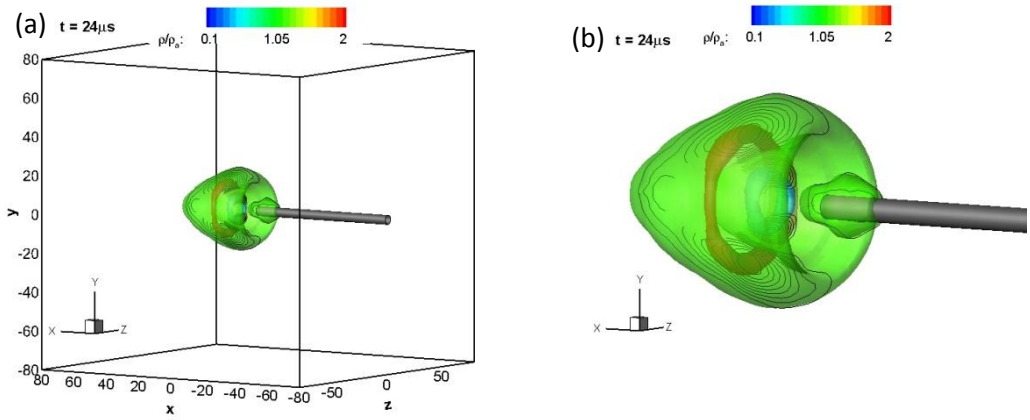

Figure 11. (a) Reconstructed density field at t = 24μs, (b) Close up view of the iso-surface of density

The relation for over density is useful in validating the density values which is obtained from BOS measurement. Using the Eq. 2, the scaled radius and time is plotted in Figure 9. The Mach number and the thermodynamic properties are plotted in Figure 10.

3.1.5 Reconstruction of the density field

The density gradient field can now be used as the input to calculate the density field. The constant of integration needed after solution of the Poisson equation is obtained by using the ambient density which is known. The 3D density field is then reconstructed using the Filtered Back Projection technique. Figure 11 presents the reconstructed three dimensional density field of the flow for time instants of 24, 53, 93, 122 and 127μs. The density values are plotted in surface contours with appropriate translucency and with a center plane slice showing the line contours. The iso-surface values of the density are clearly indicated for easy understanding of the flow features of the spherical wave front. The density values obtained through the reconstruction are normalized with the ambient density values. The reconstructed density values are actually the over density values for the given flow.

At time t = 24μS, the density field exhibits two major features as shown in Figure 11(a). One of the features is a strong

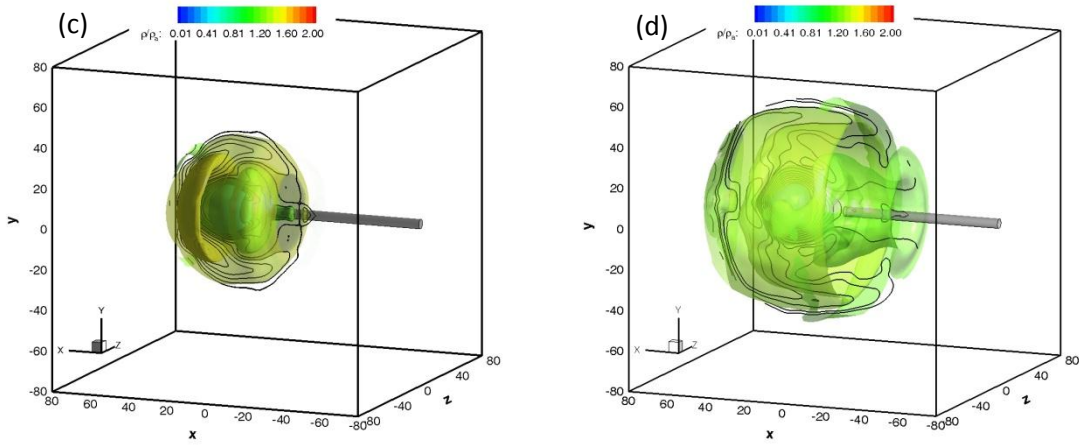

Figure 11. Reconstructed density field at (c) t = 53μs and (d) t = 93μs

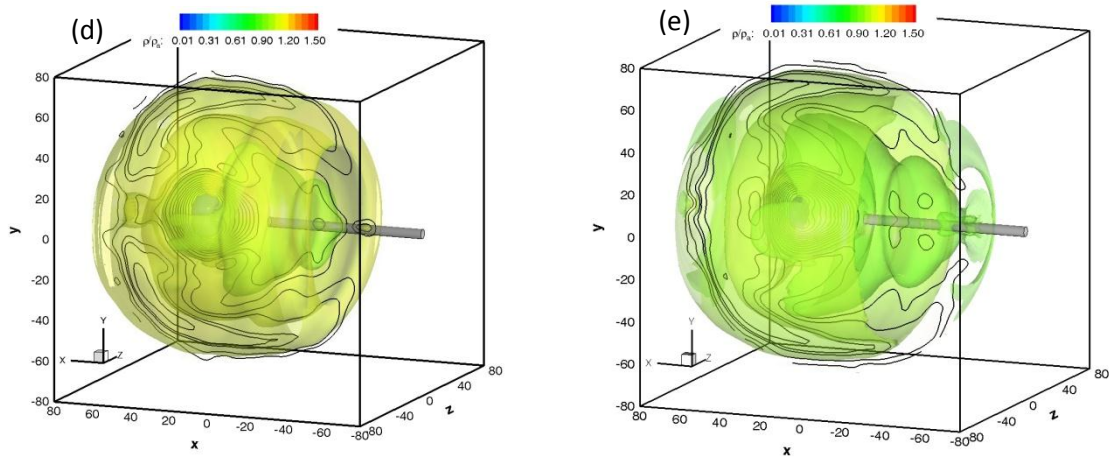

Figure 11. Reconstructed density field at (e) t = 122µs and (f) t = 127µs

ring shaped region of higher density and the advancing shock wave front is partially obscured by the large flash as remarked before. It is difficult to comment on the spherical nature of the blast wave and on the accuracy of the density field in that region. Additionally the outer most surface of the blast wave exhibits a shape that is similar to that shown in Kliene et al. [12].

The combustion happens between the inner walls of the cylindrical NONEL® tube. These combustion products when exiting the tube provides directionality to the flow along the axis of the tube. Figure 11 (a) and 11 (c) shows the axial velocity dominance and clearly emphasize that this flow is not truly a point explosion. Similar nature of the flow is seen in the work of Kliene et al. [12]. The chemical detonation process creates a rapid release of energy which produces gases of high pressure and high temperature. Since the energy release is so rapid, the expansion of gases in the ambient produces an expanding spherical shock wave which attains higher order of spherical nature quickly (Dewey [5]. Figure

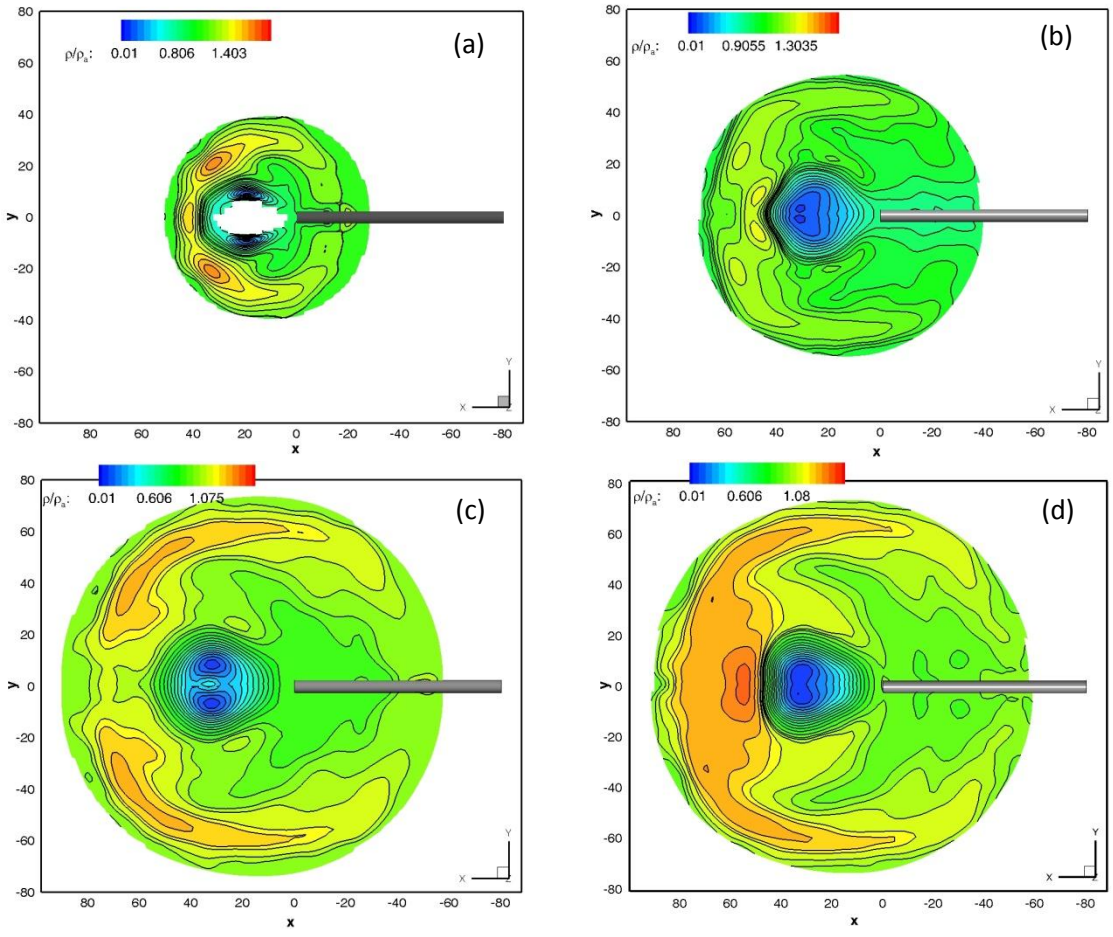

Figure 12. 2D slices at Z = 0mm (a) t = 53µs, (b) t = 93µs, (c) t = 122µs and (d) t= 127µs.

11 (c) shows the shock wave attaining a spherical shape within a short duration of time.

After burning of the Un-burnt HMX occur and this continues to produce energy at the back of the shock wave. The temperature measured at the exit of the tube is about 6000K (Hegde et al. [10]). The contact surface is very unstable and this produces considerable turbulent mixing between the combustion gases and the ambient air. The contact surface between these gases and ambient is irregular and can also be seen in the density gradient field shown earlier in Figure 6. Figure 11 (d) shows the axial velocity component of the vortex core is reduced and it expands in the transverse direction due to the transverse flow of energy and mixing process.

2D slice extracted at Z = 0mm from the reconstructed 3D over density field at various time instants are shown in Figure 12. The vortex ring which is formed grows in diameter till t = 53µs, and then decreases in size at t = 93µs as seen in Figure 12 (b). Extent of the vortex ring again grows in size at t = 122µs and then it decreases in size. The chemical combustion of the un-burnt HMX expands at a faster rate while the vortex ring accelerates in the forward direction. Due to the presence of the shock front and the expanding gases, the vortex ring region is unable to propagate forward and then grows transversely. The energy provided to the ring reduces as the combustion process is near complete and the ring reduces in size.

The 2D slices also help us in determining the uniformity in the strength of the shock wave. Uniformity in the strength of the shock wave is determined through polyline extraction in the horizontal and vertical direction. Over Density values obtained through polyline extraction of the 2D contour plot at t = 53µs is shown in Figure 13. Data is extracted along the axis of flow at a small angle to the *x*-axis. This is done to ovoid data loss due to presence of the steel tube itself. Figure 13 shows there is a slight asymmetry in the shock strength compared to the forward and the rearward propagating portion of the shock. Similar trend is seen at other time instant also. The strength of the shock at the rearward side is reduced by about 30% when compared with that of the leading edge. The asymmetry in the strength of the shock wave is not captured in any of the experimental methods carried out for the blast waves generated from micro-explosions. The density behind the shock wave will be of higher magnitude, while there is significant region of lower density. The exit temperature of 6000K [10] at the center portion of the flow and expansion of gases may be the reason for the presence of the lower density as shown in Figure 12. This could be a limitation of the technique to quantify the density in the regions of higher temperature.

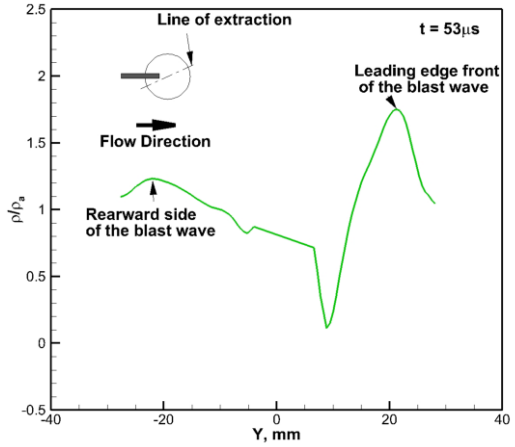

Figure 13. Comparison of the shock strength by density rise across shock

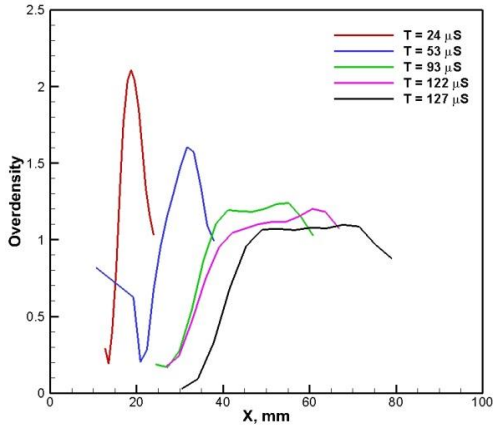

Figure 14: Extracted density values from reconstructed density field

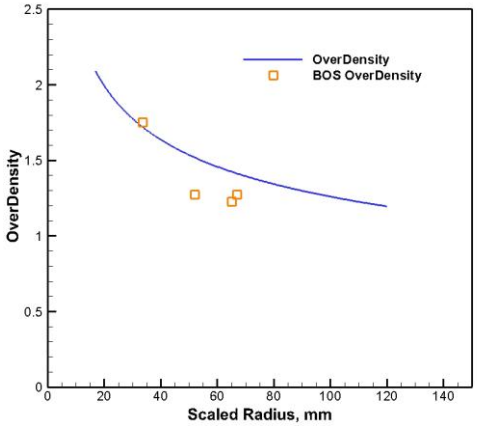

Figure 15: Comparison of the over density values from BOS and Rankine-Hugoniot relations

In order to estimate the shock strength variation during the evolution of the shock wave, density values are extracted from the 2D slice and are plotted in Figure 14. The strength of the shock decreases as it evolves over distance and can be seen from the values of over density plotted in Figure 14. The evolution of the density over time shows a similar trend to that of the numerical simulation on the micro-explosions by Jiang et al. [11].

The peak over density values behind the shock wave obtained through BOS and R-H relations (Figure 15) do not match well, except at t = 24μS. The reason for the mismatch in the overdensity values is yet to be ascertained.

3.2 PIV measurements

The results from the PIV measurements were shown in Figure 15 at several instants of time. The velocity of the blast wave front is of importance, as it can be used to determine the properties behind the blast wave. This could be a validating case for the BOS experiments. Larger instants of times were used in order to capture the blast wave front. The intensity of light scattered from the seeding particles were far less compared to that of the alumina particles created

Figure 15: PIV images at t = 155, 160, 203 and 234 μs

from the products of combustion at the center. The reason could be that the data acquisition software automatically adjusts the intensity threshold towards the high intensity alumina particles. This reduces the signal to noise ratio of the seeding particles in the ambient, when compared to the alumina particles at the core. The blast wave front is not captured in any of the runs done. However the fact that the vortex core is visualized shows that the flash from the explosion has not overcome the laser sheet, else only a diffuse blob would have been seen. The use of solid highly reflective seeding particles and alternate way of seeding the flow are currently being explored. These efforts could improve the light scattered from seeding particles near the blast wave front.

3.3 Repeatability and measurement uncertainty

The uncertainty due to the tube length was about ±0.8mm over 32 experimental data points. Jitter in the wave front coming out of the exit of the tube was about ±20 μS. The uncertainty in the curve fit to obtain radius is about ±0.5 mm. The sensitivity of the experiment for the given density gradient is found to be 0.76.

4. Conclusion

BOS measurements were carried on a micro-explosion to capture the density field. These studies show BOS technique can be employed in a spatio-temporally varying flow. The study also provides quantitative information which is not possible through other diagnostic tool on these types of transient flows. Even though previous researchers have used BOS for their studies, comprehensive quantitative density field measurements through BOS are missing. This experimental study is unique and uses BOS technique to completely characterize the density field of a micro-explosion. The asymmetry in the strength of the shock wave is not captured in any of the experimental methods carried out for the blast waves generated from micro-explosions. Comparison of the density values obtained through BOS experiments and through Rankine-Hugoniot relations does not match well as expected. PIV measurements failed to yield meaningful velocity field due to the saturation caused by the alumina in the blast. An alternate highly reflective seeding the ambient in place of the liquid droplet seeding is required. In the regions of higher temperature, the BOS technique suffers limitation in quantifying the density values. The study shows enormous potential of BOS data for both density as well as validation of CFD models.

Acknowledgement: The authors acknowledge the support provided by K Prasada Rao and Nitin Prakash Pawar in designing and fabricating the timing circuit for the experiments. The technical and the support staff of 0.55 Low speed Laboratory, help is acknowledged.

References

1. Arakeri JH, Das D, Krothapalli A, Lourenco L, “Vortex ring formation at the open end of a shock tube: A particle image velocimetry study”, Physics of fluids 16(4), 1008 – 1019, 2004.
2. Baird JP, “Supersonic vortex ring”, Proc. R. Soc. Lond. A 409: 59-65, 1987.
3. Baker WE, “Explosions in Air”, University of Texas Press, Austin and London, 1973.
4. Kenny GF, Graham KJ, Explosive Shocks in Air, 2nd Edition. Springer-Verlag, NewYork, 1985.
5. Dewey JM, “Expanding Spherical Shocks (Blast Waves)”, In: Ben-Dor G, Igra O, Elperin T (eds.) Handbook of Shock Waves”, Vol. 2, Academic Press, chap .13.1, pp 441–48, 2001.
6. Dewey JM, “The properties of a blast wave obtained from an analysis of the particle trajectories”. Proc Roy Soc A 324: 275–299, 1971.
7. Dewey JM, “Air velocity in blast waves from TNT explosions”, Roy.Soc.- Proc. Ser.A 279 (1378), 366–385, 1964.
8. Dewey JM, “Explosive Flows: Shock Tubes and Blast Waves. In: W-J Yang (ed.): Handbook of Flow Visualization”, Taylor and Francis, chap. 29, 481–497, 1989.
9. Hargather MJ, Settles GS, "Optical measurement and scaling of blasts from gram-range explosive charges", Shock Waves, 17:215–223, 2007.
10. Hegde G, Pathak A, Jagadeesh G, Oommen C, Arunan E, Reddy KPJ, “Spectroscopic studies on micro-explosions”, Proceedings of the 27th International Symposium on Shock Waves, Russia, 2009.
11. Jiang Z, Takayama K, Moosad KPB, Onodera O, Sun M, “Numerical and experimental study of a micro-blast wave generated by pulsed-laser beam focusing”, Shock Waves, 98 Vol. 8: 337349, 1998.
12. Kleine H, Dewey JM, Ohashi K, Mizukaki T, Takayama K, “Studies of the TNT equivalence of silver azide charges”, Shock Waves 13: 123–138, 2003.
13. Murphy MJ, Adrian RJ, "Particle response to shock waves in solids: dynamic witness plate/PIV method for detonations", Experiments in Fluids, 43:163–171, 2007.
14. Sommersel OK, Bjerketvedt D, Christensen SO, Krest O, Vaagsaether K, “Application of background oriented Schlieren for quantitative measurements of shock waves from explosions”, Shock Waves 18:291–297, 2008.
15. Mizukaki T, Tsukada H, Wakabayashi K, Matsumura T, Nakayama Y, "Quantitative Visualization of Open-Air Explosions by using Background-Oriented Schlieren with Natural Background", Paper No 2564, Proceedings of the 28th International Symposium on Shock Waves, Manchester, UK, 2011.
16. Oommen C, Jagadeesh G, Raghunandan BN, “Studies on micro explosive driven blast wave propagation in confined domains using NONEL tubes”, Proceedings of the 26th International Symposium on Shock Waves, Gottingen, Germany, 2007.
17. Obed SI, Jagadeesh G, and Kontis K, “Micro-Blast Waves Using Detonation Transmission Tubing”, Proceedings of the 27th International Symposium on Shock Waves, Russia, 2009.
18. Suriyanarayanan P, Karthikeyan N, Venkatakrishnan L, Obed SI, Sriram S, Jagadeesh G, “Density field measurement of a micro-explosion using BOS”, Paper No 2452, Proceedings of the 28th International Symposium on Shock Waves, Manchester, UK, 2011.
19. Venkatakrishnan L, Meier GEA, “Density measurements using background oriented Schlieren technique”. Experiments in Fluids, 37(2):237– 247, 2004.
20. Venkatakrishnan L, Suriyanarayanan P, “Density field of supersonic separated flow past an afterbody nozzle using tomographic reconstruction of BOS data. Experiments in Fluids, 47(3), 463-473, 2009.